Advanced Diamond-reinforced Metal Matrix Composites via Cold Spray: Properties and Deposition mechanism

Shuo Yin[a*], Yingchun Xie[b], Jan Cizek[c], Emmanuel Ekoi[d], Tanvir Hussain[e], Denis Dowling[d] and Rocco Lupoi[a*]

a. Trinity College Dublin, The University of Dublin, Department of Mechanical and Manufacturing Engineering, Parsons Building, Dublin 2, Ireland
b. Université Bourgogne Franche-Comté, Université de technologie Belfort-Montbéliard, LERMPS, 90010, Belfort, France
c. Netme Centre, Institute of Materials Science and Engineering, Brno University of Technology, Technicka 2896/2, 616 69, Brno, Czech Republic
d. University College Dublin, School of Mechanical and Materials Engineering, Belfield, Dublin 4, Ireland
e. University of Nottingham, Division of Materials, Mechanics and Structure, Nottingham NG7 2RD, UK

Abstract: Diamond-reinforced metal matrix composites (DMMC) have great potential for wear-resistance applications due to the superior hardness of the diamond component. Cold spray as an emerging coating technique is able to fabricate coatings or bulk materials without exceeding the material melting point, thereby significantly lowering the risk of oxidation, phase transformation, and excessive thermal residual stress. In this paper, thick DMMC coatings were deposited onto aluminum alloy substrate via cold spray of three feedstock powders: copper-clad diamond and pure copper, and their mixtures. It was found that, due to its low processing temperature, cold spray is able to prevent graphitization of the diamond in the DMMC coatings. Further to that, the original diamond phase was almost completely retained in the DMMC coatings. In case of the coatings fabricated from copper-clad diamond powders only, its mass fraction reached 43 wt.%, i.e. value higher than in any previous studies using conventional pre-mixed powders. Furthermore, it was found that the added copper content powders acted as a buffer, effectively preventing the fracture of the diamond particles in the coating. Finally, the wear test on the coatings showed that the cold sprayed DMMC coatings had excellent wear-resistance properties due to the diamond reinforcement.

Keywords: Kinetic spray, microstructure, tribology, finite element analysis, modeling

Corresponding author. Email: yins@tcd.ie (Shuo Yin); lupoir@tcd.ie (Rocco Lupoi)

1. Introduction

Diamond is known to possess extremely high hardness, allowing it to be used as an excellent wear-resistance material. However, for the same reason, it is difficult to be machined, which in turn limits its direct applications. To overcome the limitations, diamond is normally applied in a form of thin, wear-resistant coatings. Chemical vapor deposition (CVD) technique can be used to produce such films. However, CVD films are restricted in terms of thickness, frequently suffer from low toughness, and tend to crack or peel off completely from the substrate due to the large thermal and residual stress generated during their solidification [1,2].

Diamond-reinforced metal matrix composites (DMMC) are novel materials in which the metallic phase acts as a binder (yielding the DMMC deformable and machinable), while the reinforcement diamond phase helps to improve the material properties. Currently, the common ways to fabricate bulk DMMC are powder metallurgy [3–7] and pressure infiltration techniques [8–12]. These methods mostly require extremely high processing temperatures to melt the metal binder, thereby significantly increasing the risk of the metal phase transformation and diamond graphitization, which, in turn, may potentially yield inferior material performance [5]. In terms of DMMC thin films for wear-resistance applications, various thermal spray techniques such as oxy-acetylene thermal spray [13–15], HVOF [15], supersonic laser deposition [16,17], and laser cladding [17] were applied. Analogous to the powder metallurgy and pressure infiltration techniques for producing bulk DMMC, these thermal spray techniques also require high working temperatures and the films/coatings therefore potentially face identical problems (in particular, graphitization of the diamond content [17]). Higher diamond contents in the coatings is known to improve the coating wear-resistance by reducing the wear rate [13]. However, in the thermally sprayed coatings, the diamond content is usually much lower than the binder phase content. Combined, these disadvantages

47 significantly lower the wear-resistance properties of the thermally sprayed DMMC coatings. Therefore, it is
48 rather meaningful to develop a novel fabricating method of DMMC coatings that would avoid the risk of
49 diamond phase graphitization and simultaneously retain high diamond contents.

50 Cold spray as an emerging coating technique is capable to deposit metals, MMC [18–20] and even
51 ceramics [21,22], thereby attracting great interests over the last decades [23]. In this process, feedstock
52 materials in the form of micron-sized powders are accelerated by a supersonic gas passing through Laval
53 nozzle, and subsequently impact onto a substrate to form the coating [24–27]. During the deposition process,
54 the feedstock remains solid state without any melting; the coating is formed through a metallurgical or
55 mechanical bonding at the interface of adjacent particles and coating/substrate. Thereby, difficulties and
56 defects such as oxidation, detrimental thermal residual stress development, and phase transformations which
57 commonly appear in powder metallurgy, pressure infiltration, or thermal spray processes can be
58 considerably avoided [28]. Furthermore, the coatings in cold spray can be deposited onto various substrates
59 (such as metals, polymers, ceramics) and the respective thickness growth is almost unlimited for most
60 metals and MMC, allowing cold spray to act as an additive manufacturing technique for producing bulk
61 materials [29,30].

62 To date, very few attempts of cold spraying of DMMC coatings for improving the hardness and Young's
63 modulus have been carried out [31,32]. The state of the art suggests that the limitation for fabricating
64 DMMC (also applicable for other MMC) via cold spray is the feedstock powders. Typically, either
65 mechanically pre-mixed or ball milled feedstock is used. However, using the pre-mixed powders frequently
66 leads to a reduction of the diamond phase content in the coating as compared to the original feedstock due to
67 the its low deposition efficiency, while the ball-milling procedure in turn results in a serious fracture of the
68 diamond phase or its graphitization [31,32]. Aside from reducing the cost efficiency of the process through

69 the loss of diamond powder in such case, the coating performance is significantly lowered, too [16,17,33].

70 In this paper, DMMC coatings were fabricated via cold spray technique. In order to avoid the
71 disadvantages and problems associated with using the conventional pre-mixed or ball-milled feedstock, a
72 novel copper-clad diamond powder (and its mixture with copper powder) was used as the feedstock to
73 fabricate the coatings instead. In the previous work, this copper-clad diamond powder has been proven to
74 significantly increase the diamond contents in the coating [34]. As the base material, copper was selected
75 due to its ease of deposition and high deposition efficiency, allowing it to be an excellent binder in the MMC
76 coatings. Wear test of the fabricated DMMC coatings was further carried out to investigate the coating
77 wear-resistance capability. With copper not being a typical wear-resistance metal, the results better reflect
78 the role of the diamond reinforcement. In the future work, using typical wear-resistance metals such as
79 cobalt and nickel is planned.

80 **2. Experimental methodology**

81 **2.1. Coating fabrication**

82 Pure copper (-38+15 μm, > 99.9%, Safina, Czech Republic) and copper-clad diamond (-53+45 μm, PDA
83 C50, Element-Six, Ireland) powders and their respective mixtures were used as the feedstock. Fig. 1a-b
84 shows the morphology of both powders observed by SEM (Carl Zeiss ULTRA, Germany). The copper-clad
85 diamond powder particles typically consist of three different layers: a diamond core enclosed in a thin nickel
86 inter-layer and an outside electroless copper cladding, as can be seen from the powder cross-section shown
87 in Fig. 1c (FIB, DB235, FEI Strata, USA). The nickel inter-layer is used due to its superior bonding with
88 diamond as compared to copper. According to the supplier, the weight ratio of the diamond phase to both
89 metals in a single particle is approximately 1:1, and thus the diamond core diameter was calculated as
90 roughly between 40 and 47 μm.

The annotation of the produced coatings as well as the respective feedstock information and cold spray deposition conditions are provided in Table 1. The benchmark coating denoted as 'P0' was fabricated from pure copper powder only, i.e., no copper-clad diamond phase was present. The coatings were deposited onto common aluminum alloy substrates using an in-house cold spray system (Trinity College Dublin, Ireland). The system consists of high pressure nitrogen/helium gas from cylinders, gas heater, powder feeder, CNC working platform for controlling the substrate movement, Laval nozzle and a computer control system. In this work, nitrogen was used to produce P0 coating under previously optimized parameters, while helium was applied to produce the DMMC coatings. Each coating was fabricated with two gun passes at a robot arm traversal speed of 15 mm/s. A schematic of the cold spray coating fabrication process is shown in Fig. 2.

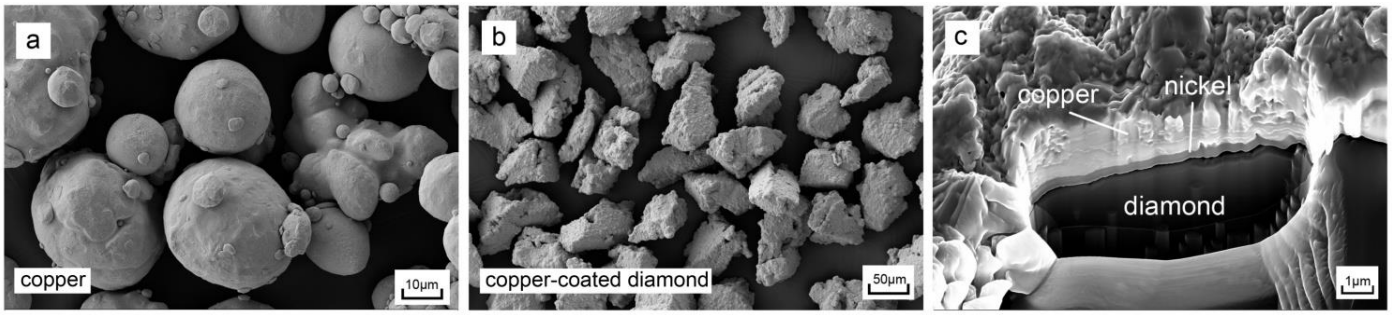

Fig. 1 Morphology of the (a) copper and (b) copper-clad diamond powders used in this study. (c) cross-section of typical copper-clad diamond particle.

Table 1 Annotation of the produced coatings, the respective feedstock composition and cold spray deposition conditions.

Coating	Feedstock powders	Gas	Pressure [MPa]	Temperature [°C]	Gun speed [mm/s]	Standoff distance [mm]
P0	Copper	N_2	3.0	350	15	45
P1	Copper + copper-clad diamond (8:1 by weight)	He	2.0	25	15	45
P2	Copper + Copper-clad diamond (1:1 by weight)	He	2.0	25	15	45
P3	Copper clad diamond	He	2.0	25	15	45

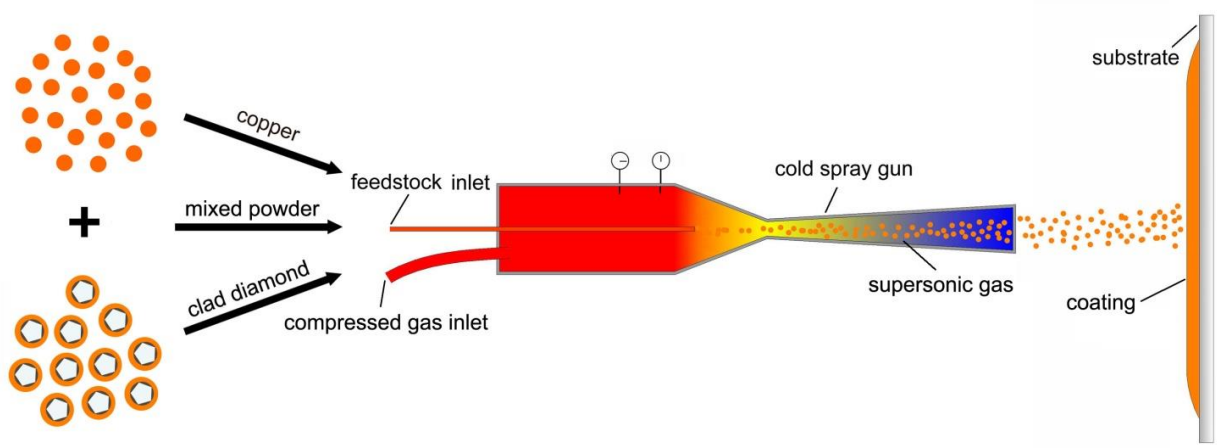

Fig. 2 Schematic of the DMMC coating fabrication via cold spray.

2.2. Materials characterization

To examine the phase content and the prospective graphitization of the diamond during the coating fabrication process, the as-sprayed coatings were examined by an X-Ray diffractometer (Siemens D500, Germany) with the Co (λ=1.789 Å) source at a current of 40 mA, voltage of 35 kV and scan step of 0.02°. To assess the coating microstructure via SEM, the as-sprayed coating samples were prepared using standard metallographic procedures with the final polishing applied by 0.05 μm Al_2O_3 solution. Fracture surface was also obtained by breaking the as-sprayed samples and the observed by SEM. The element analysis (primarily, the mass fractions of Cu and Ni) on the coating surfaces and polished cross-sections was performed with an EDS unit (Oxford Instruments INCA system, UK) equipping on the SEM system. Given its inaccuracy in measuring low molecular weight elements, the mass fraction of diamond was then calculated based on the results of copper and nickel. For each sample, five locations were randomly selected from the coating surface or polished cross-section and the measured data was then averaged.

2.3. Wear test

The wear properties were measured using POD-2 pin-on-disc system (Teer Coatings Ltd., UK) at room

temperature. For accurate measurement of the wear rates, the sample surfaces were polished using Al_2O_3 solution to 1 μm roughness prior to the test and the samples were then mounted on a carrier disc. A tungsten carbide ball with a diameter of 5 mm was used as a counterpart under a constant load of 4 N. The disk rotated at a linear speed of 10 mm/s for 15000 revolutions. To determine the coating and pin ball wear rates, the material volume loss was calculated according to ASTM G 99 standard [26]. The amount of wear was determined by weighing the specimens before and after the test. The respective wear rate was then calculated as the volume loss per unit load and per traverse distance.

It was reported that the mean free path between reinforcement particles is an important parameter affecting the coating wear-resistance property [25,35,36]. The mean free path was calculated by drawing a total of 10 random lines on multiple coating cross-sectional images and counting the number of intersects with diamond particles. Then, the mean free path could be calculated according to the following equation:

$$\lambda = \frac{1 - V_p}{N_L} \quad (1)$$

where N_L is the number of diamond particle intercepts per unit length of test line and V_p is the volume fraction of the reinforcing particles.

3. Numerical methodology

In order to study the powder particles deposition behavior during the coating formation process, finite element analysis (FEA) of the inter-particle impact was carried out using ABAQUS. The impact process was simplified as two particles successively depositing on the substrate in the same line. The contact pressure between the two particles was then calculated and compared with the diamond fracture stress to evaluate the diamond fracture behavior in the coating. Lagrangian algorithm with the dynamic explicit procedure was applied to build the computational model. The aluminum alloy substrate was defined as a cylinder, having a

diameter and height of 320 and 160 μm, respectively. Based on the average size of the powders used in the experiment, the copper particle was defined as a sphere with a diameter of 26 μm. For the preliminary evaluation, the irregular copper-clad diamond powder was simplified as a sphere of an equivalent diameter of 50 μm. Of that, the diameter of the diamond core and the thickness of the nickel inter-layer and copper cladding were defined as 44.5, 0.4 and 2.4 μm, respectively, in accordance with the composition information of the real powder. The metal materials including nickel, copper and aluminum alloy were modeled using Johnson and Cook plasticity model. The diamond was considered as a linear elastic model with high elastic modulus [37]. The model inherently does not allow considering the fracture of the diamond, but the maximum contact pressure between the particles can be obtained. Detailed materials parameters applied to both models can be found elsewhere [37,38]. Fig. 3 shows the computational domain, meshing and boundary conditions of the used FEA model. Due to its symmetric character, the model was simplified as axisymmetric in order to reduce the computational time. The geometry was partitioned by four-node bilinear axisymmetric quadrilateral elements with reduced integration and hourglass control (CAX4R). The axisymmetric condition was applied to the axis and the fixed boundary condition was enforced to the bottom and lateral. The contact process was implemented by using the surface-to-surface penalty contact algorithm with balanced contact pair formulation. The particle impact velocities for copper and copper-clad diamond at the applied spray conditions (Table 1) and nozzle geometries were calculated as 600 m/s and 480 m/s in a separate study (ANSYS-FLUENT 14.1 [39]).

The used FEA model inherently does not comprehend all experimental details and differs from reality in several aspects, such as in-line impact, spherical particles or not taking into account the potential out-of-equilibrium conditions of the particle materials arising from their fabrication routes (such as e.g. cold working, internal stresses, etc). As such, the model could not work (and was not used) to properly explain

e.g. the deformation mechanisms or materials flow. However, the model's features suffice to achieve the main aim, i.e. to calculate the level of stresses achieved at the contact and compare those with the diamond fracture stress values.

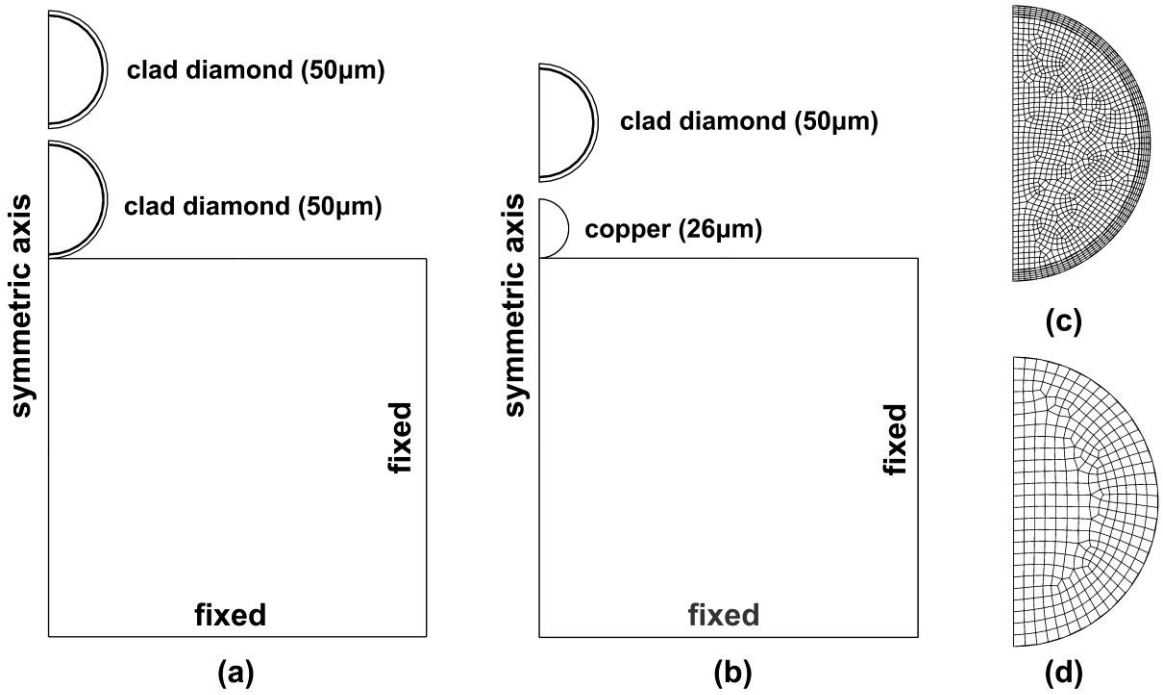

Fig. 3 Computational domain, meshing and boundary conditions of the FEA two-particle subsequent impact model. (a) two copper-clad diamond particles, (b) copper and copper-clad diamond particles, (c) mesh for copper-clad diamond powder and (d) mesh for copper powder.

4. Results and discussion

4.1 Chemical and phase transformations of DMMC coatings

The cold sprayed coatings thickness exceeded 5 mm in all cases, i.e. order of magnitude higher than what is possible to obtain using vapor deposition processes. As the mass fraction of the copper-clad diamond feedstock increased (i.e., the copper content decreased, from P0 to P3), the coating color changed from copper red to gray. Fig. 4 shows the copper content on the P0-P3 coating surfaces as determined by EDS as

177 well as the corresponding sample appearance.

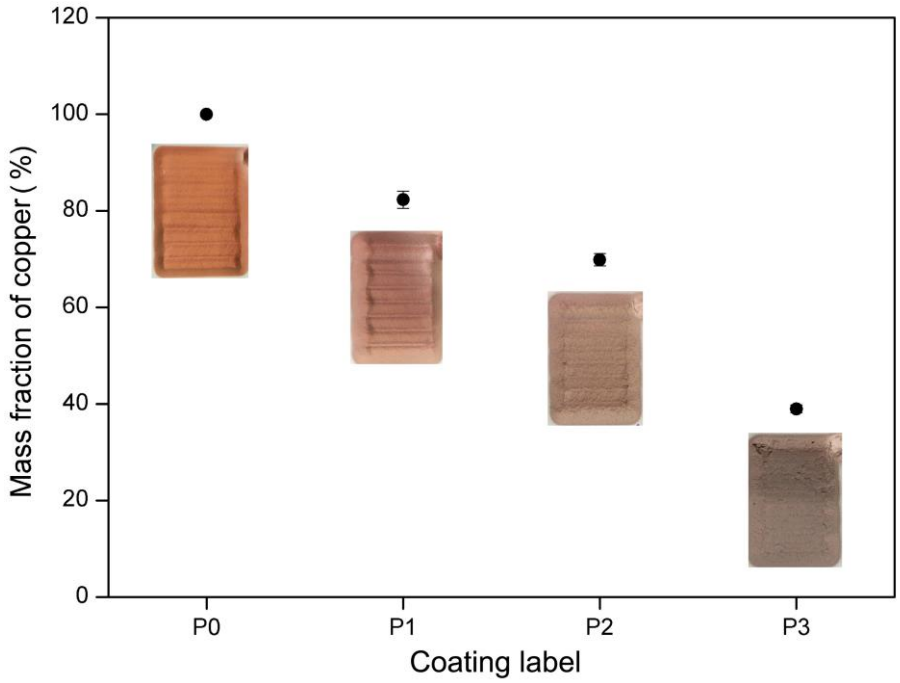

178

179 **Fig. 4** Copper content (wt%) on the P0-P3 coating surfaces as determined by EDS.

180 Graphitization of the diamond frequently occurs when fabricating the DMMC via sintering, infiltration
181 or thermal spray techniques due to the high processing temperatures [4,5,16,17]. The obtained XRD spectra
182 in Fig. 5 showed no graphite peaks, indicating that no graphitization occurred during the fabrication of the
183 cold sprayed DMMC. This fact clearly shows the advantage of cold spray over the other fabrication
184 techniques in preventing diamond graphitization. Moreover, the spectra presented in Fig. 5 further suggested
185 an increasing content of nickel and diamond phases from P1 to P3. This was supported by EDS cross-section
186 analysis of the diamond content (Fig. 6). The coating P3 that was fabricated from copper-clad diamond
187 powder only (50 wt% of diamond phase) contained 43 wt.% diamond, suggesting its fairly high deposition
188 efficiency in the process. In our previous work, even higher value of 56 wt.% was obtained by the EDS
189 measurements. However, it is rather safe not to attribute the difference to a change in deposition efficiency
190 as the higher value was obtained from coating fracture (i.e., not polished) surfaces [34]. In the previous cold

spray works where mechanically pre-mixed metal and diamond powders were used as the feedstock [33,40,41], most of the diamond could not successfully deposit and thus the diamond mass fraction in the coatings was generally low. The diamond fraction obtained in our works is higher than in any previous studies using conventional pre-mixed powders. The excellent performance of the copper-clad diamond powder clearly indicates that it is a promising feedstock for fabrication of cold sprayed DMMC coatings.

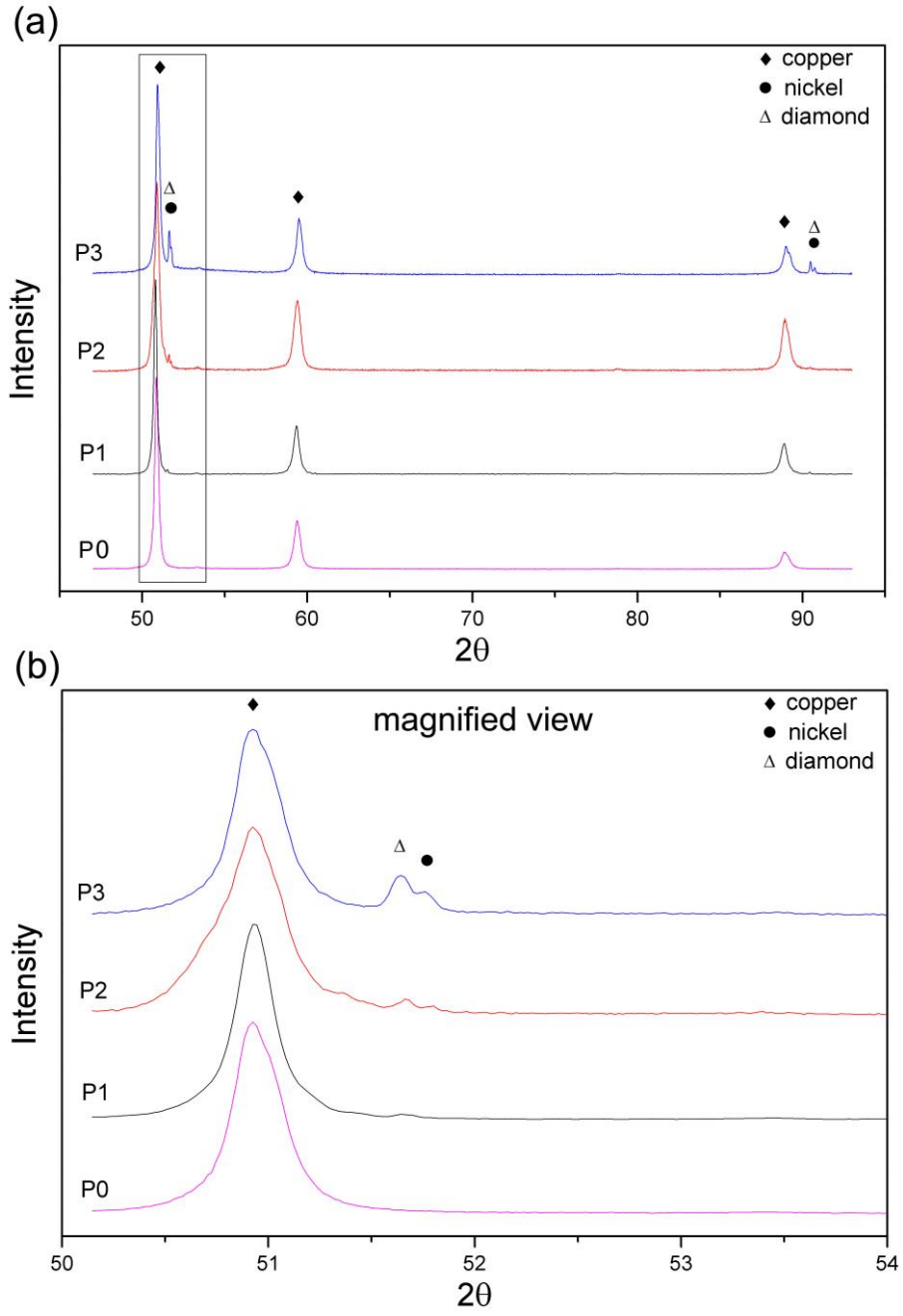

Fig. 5 Comparison of the XRD spectra of the produced P0-P3 coatings (a) and local magnified view marked by black square in Fig. 5a (b). Note the increasing content of Ni and diamond phases toward P3.

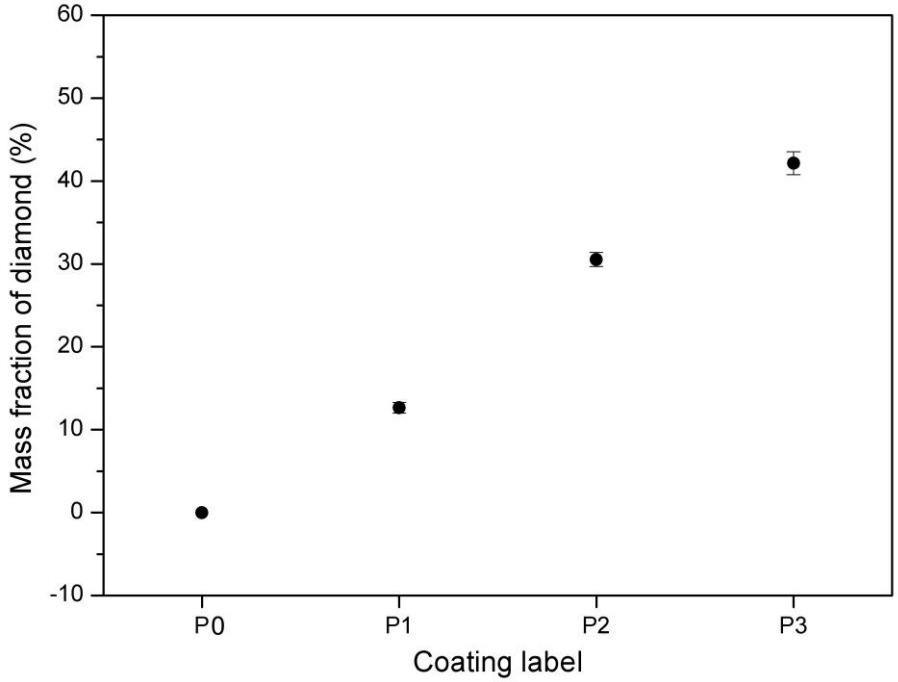

Fig. 6 Mass fraction of diamond on the coating cross-section.

4.2 DMMC coating microstructure

Fig. 7 shows the cross-sectional features of the DMMC coatings fabricated using different powders. It is known that a uniform distribution of the reinforcement phase in the MMC is of great importance to the final materials properties [42–44]. In this work, the cold sprayed DMMC coatings fabricated with the copper-clad diamond powders exhibited excellent uniformity, providing an essential condition for the high-quality materials properties. Besides, an obvious difference in the diamond mass fraction between each sample can be seen. The observed diamond contents in the coatings (P3 > P2 > P1) were well consistent with the EDS element analysis shown in Fig. 6.

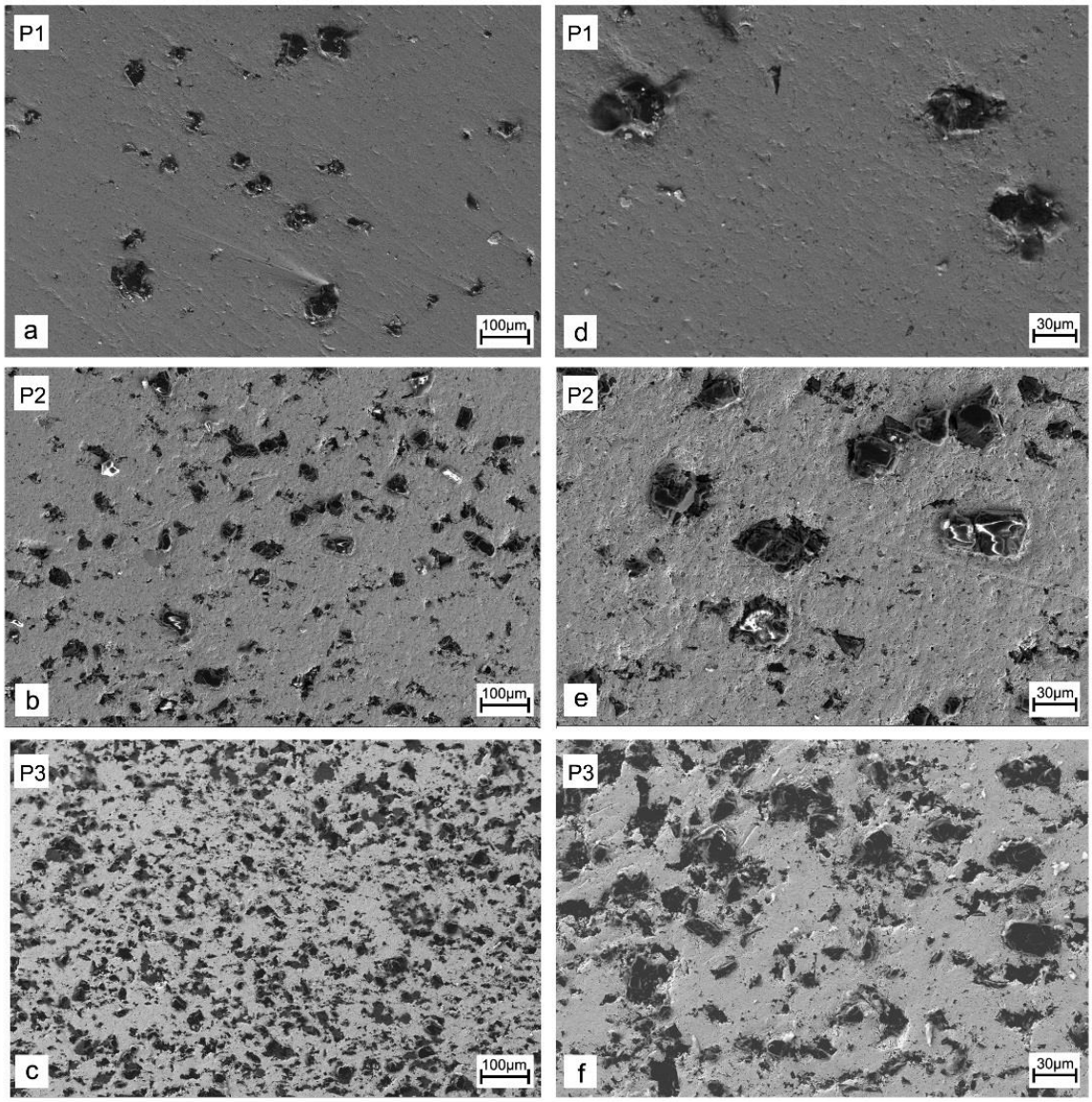

Fig. 7 Microstructure of the produced P1(a,d), P2 (b,e), and P3 (c,f) cold sprayed coatings.

The magnified images of the cross-section provided in Fig. 7d-f illustrate the diamond particles sizes in the produced coatings. Most of the diamond in the coating fabricated with the P1 and P2 powders had a diameter of approximately 40µm. This value was quite comparable to the diamond core diameter of original feedstock (-47+40 µm), which indicated that diamond did not exhibit substantial fracturing during deposition. In fact, the diamond phase in P1 exhibited almost no damage, while few cracks and several small diamond shards only could be found in P2. Assumedly, the matrix consisting of the free copper powder particles provided ductile component absorbing the impact energy and thereby effectively preventing the

diamond phase fragmentation. However, in the case of P3 coating, which was fabricated entirely using copper-clad diamond powder only, the diamond phase was considerably smaller, containing a large number of diamond shards with a diameter of less than 10 μm, suggesting the occurrence of fracturing. Despite the fracture, previous works reported that tiny shards or fine particles may improve the toughness of cold sprayed composite coating [19,20].

For well explaining the reason for inducing diamond fracture behavior in the pure copper-clad diamond coating, Fig. 8 shows the predicted stress distribution at the moment of (i.e., at the precise moment when the nominal stress reaches its maximum during the entire process) a copper-clad diamond powder impact (onto either copper or copper-clad diamond particles), with room-temperature helium under 2.0 MPa pressure as the propellant gas (i.e., identical to spraying conditions). For P1 and P2 coatings, the soft copper particles could act as a ductile matrix to the copper-clad diamond particles, dissipating most of the impact kinetic energy through the plastic deformation of copper. The predicted maximum impact stress in such case (Fig. 8a) reached almost 3900 MPa, i.e. significantly lower than the diamond fracture stress calculated elsewhere (5900 MPa, [37]). Therefore, the impacting stress was unlikely to damage the diamond in case of impact into the copper matrix. The minor fragmentation of the diamond phase observed in P2 coatings (considerably lower than in P3 coatings, nevertheless; cf. Fig. 7e and 7f) could be caused by a prospective diamond-diamond contact given its higher content as compared to P1 coating. For P3, the outside metal cladding was very thin and most of the energy was directly imposed on the inner diamond cores due to the absence of softer buffer materials. The impact stress reached 8900 MPa (Fig. 8b). In this case, most of the diamond was certainly fractured during the deposition, in accordance with the observed microstructure (Fig. 7c,f).

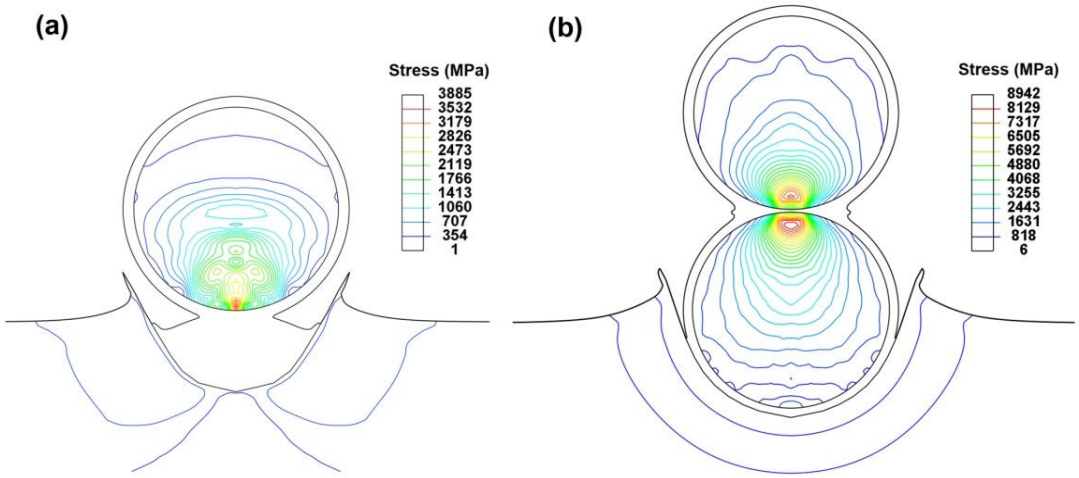

Fig. 8 FEA modeling results of the stress distribution at the moment of particle-particle impact with the inlet pressure of 2.0 MPa and helium as the propulsive gas. (a) copper-clad diamond onto copper, (b) copper-clad diamond onto copper-clad diamond

To further observe the coating microstructure and clarify the diamond phase behavior, coating fracture surfaces were observed using SEM (Fig. 9). The diamond particles in P1 coating were complete without any visible signs of damage, while the P2 coatings contained both undamaged and slightly damaged diamonds. However, for the P3 coating shown in Fig. 9c, the diamond phase observed a frequent cracking, producing small diamond shards surrounding the parent particles. In such cases, bonding occurred between the thin copper claddings only and the coating was formed through the fractured diamond sub-particles uniformly dispersing into the metal phase [34].

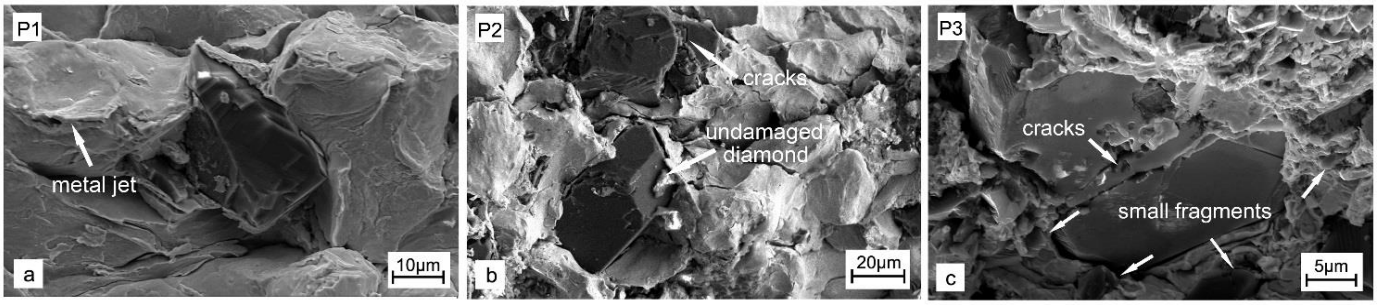

Fig. 9 Fracture surfaces of the produced P1-P3 coatings and the respective diamond phase fragmentation behavior

4.3 Coatings Deposition Mechanisms

Following the coating microstructure analysis, the following deposition mechanisms are suggested herein. Fig. 10 shows the schematic of the deposition mechanisms for different coating types. For the coatings produced using a mixture of copper and copper-clad diamond particles (Fig. 10a), the copper-clad diamond particles have a limited chance to impact with each other only. Instead, they mostly impact onto copper and, as a result, the metallic bonding in the coating mainly occurs between the copper particles only or between the copper claddings of the diamond cores and copper particles. In addition, as the energy caused by the high-velocity impact is mostly transformed into the plastic deformation of copper, the impact stress imposed on the diamond phase does not reach its fracture stress threshold and the entire diamond content therefore uniformly embeds and distributes in the copper phase.

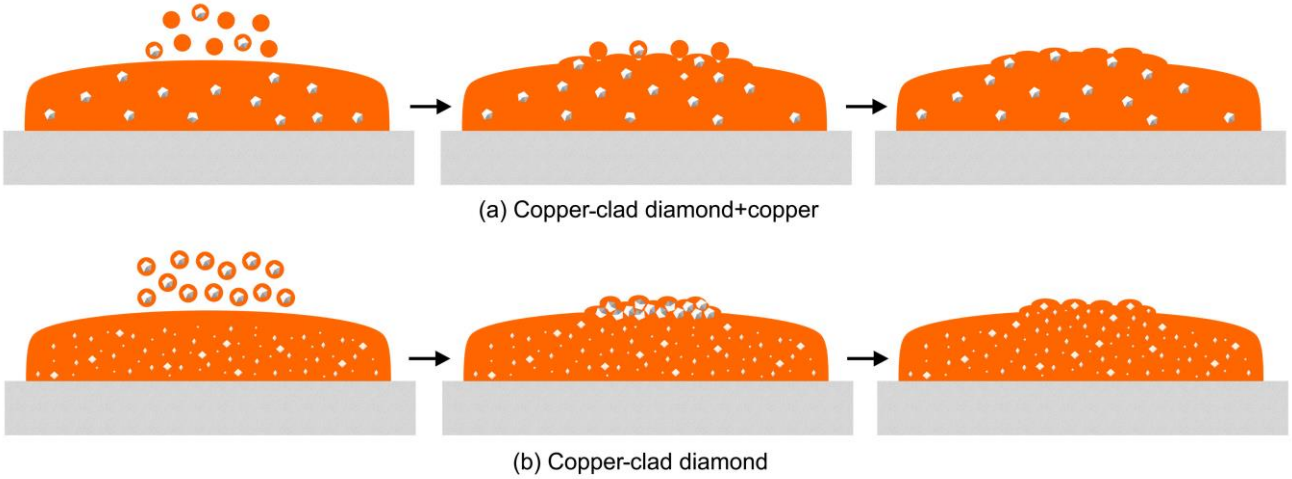

Fig. 10 Schematic of the deposition mechanisms for (a) copper-clad diamond + copper coating and (b) copper-clad coating

For the copper-clad diamond coatings (Fig. 10b), pure copper particles are absent in the deposition process, leading to impacts of the copper-clad diamond particles with each other directly. Then, the metallic bonding in the coatings only takes place between copper claddings. Although the copper cladding dissipates part of the kinetic energy through plastic deformation, it is too thin (2-5 μm) to act as a buffer. Most of the kinetic energy is dissipated via the interaction between the diamond cores rather than the plastic deformation

of the copper part. As a consequence, the impact stress imposed onto the diamond is large, exceeding the diamond fracture stress, as discussed in the last section. Diamonds hence fracture into shards during the deposition and disperse into the copper phase to form the DMMC.

4.4 Coatings Wear Test

The DMMC coatings experienced almost no wear during the test. Instead, the tungsten carbide pin ball counterpart exhibited signs of damage. Also, a large amount of black debris worn from the tungsten carbide pin ball was left on the worn track after the testing. As the debris surely affected the sample weight, the coating wear rate measurement could not be taken as valid from this test. Fig. 11 provides the measured wear rate of the tungsten carbide pin ball as a function of the calculated mean free path. It is clearly seen that the mean free path decreased from P1 to P3, while the wear rate of the pin ball increased gradually. This fact indicated that the coating wear-resistance performance steadily improved as the mean free path decreased, in good agreement with the previous work [36]. The wear rate of the pure copper coating was also measured for comparison reason. The copper coating was seriously worn after the test with the wear rate of 0.0077 mm^3/N.mm while the pin ball did not experience any significant signs of damage. The comparison clearly indicates the importance of the diamond reinforcements in improving the coating wear-resistance properties. Moreover, in the previous works related to cold sprayed wear-resistance coatings (e.g., Al5056/SiC [45], CuSn8/AlCuFeB [46]), materials loss normally occurred on the coating surface, while the wear of WC-Co pin ball was not reported. This fact further suggests the excellent wear-resistance properties of the cold sprayed DMMC coatings obtained in this work.

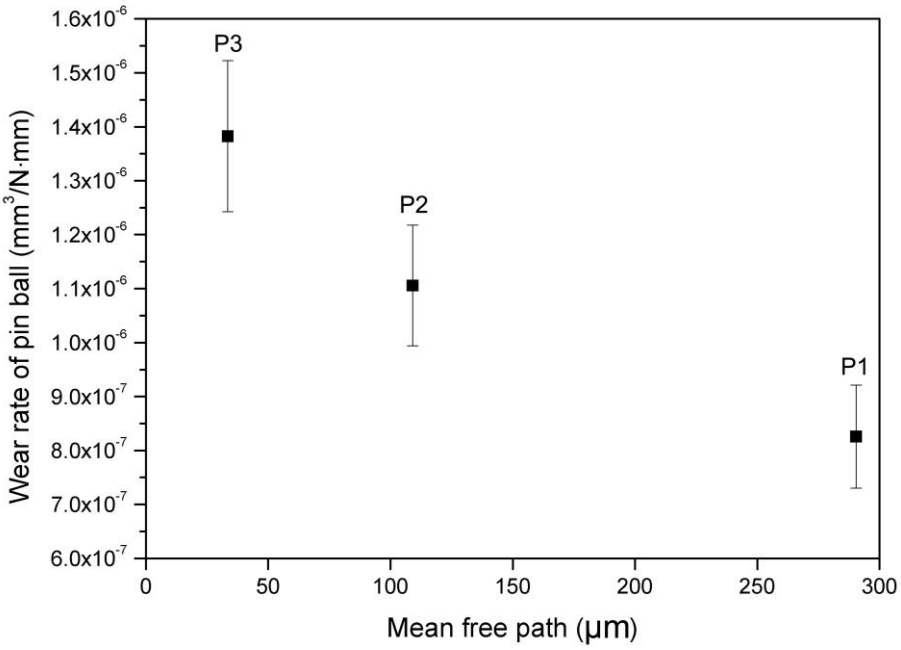

Fig. 11 Experimentally measured wear rate of the tungsten carbide pin ball against mean free path between diamond particles in the respective produced DMMC coatings.

To further investigate the coating wear mechanism, the worn surfaces and the corresponding EDS measurements are provided in Fig. 12. For the pure copper coating (P0), the worn surface was characterized by smooth profile with slight signs of delamination only. For P1 (having the lowest content of the diamond phase among P1-P3), tungsten carbide film worn off from the pin ball was detected on the worn surface. Also, the diamonds were not pulled off from but rather remained embedded in the P1 coating. They prevented the pin ball to wear the metal phase of the coating, but led to the serious abrasion of pin ball. With the pin ball continuously sliding on the coating surface, the tungsten carbide debris formed a thin film on the worn surface. As the diamond contents increased (P2), the area of the tungsten carbide film became larger (i.e., increased pin ball abrasion), lowering the area of the exposed coating materials. Therefore, the wear rate of the pin ball was higher than that of P1. In the case of P3 fabricated with copper-clad diamond powder only, a large amount of diamond resulted in the entire worn surface covered by the black and thick tungsten carbide film without any exposure of the underlying coating material whatsoever. The wear rate of the pin

ball was therefore the highest in all tests. It is known that copper is not a typical material for wear-resistance coating due to its relatively low hardness [27]. Therefore, it is plausible to suggest that the wear-resistance capability of the produced DMMC is attributed to the diamond reinforcements. The performed wear test results clearly indicate the great potential of cold spray technique for producing wear-resistance DMMC coatings.

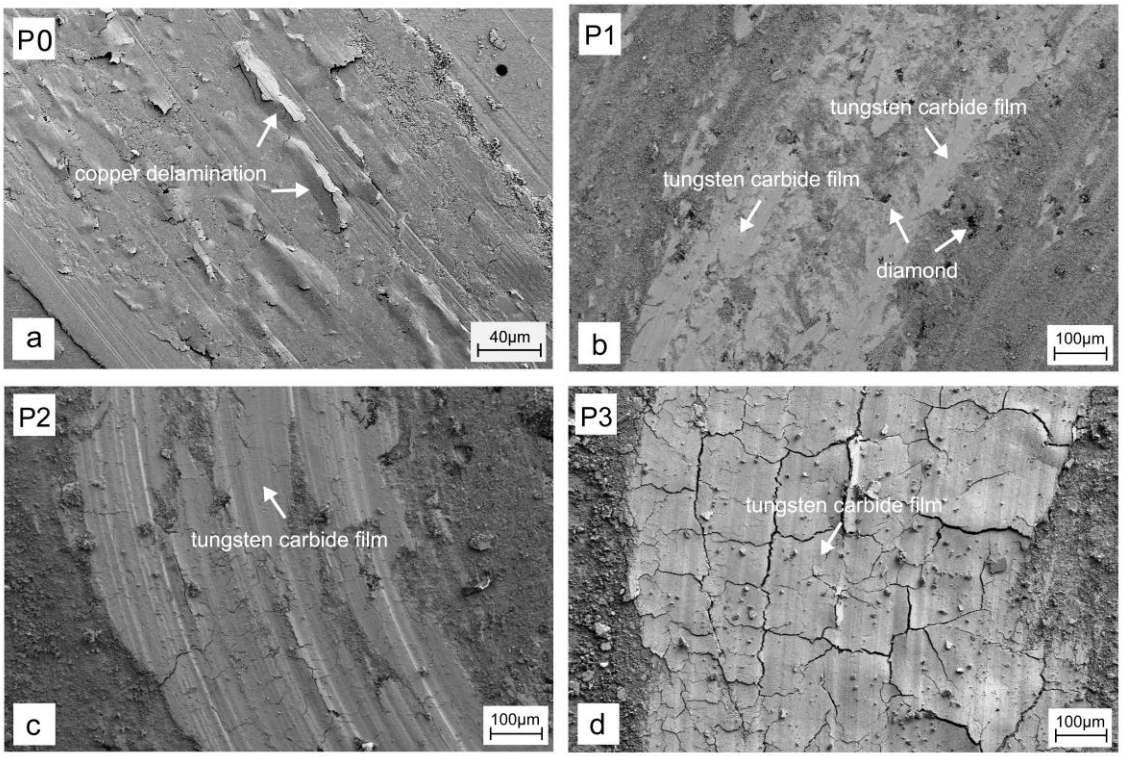

Fig. 12 SEM images and the corresponding EDS results of the worn surface of the cold sprayed P0-P3 coatings.

Conclusions

In this paper, a range of diamond-reinforced metal matrix composites (DMMC) were fabricated via cold spray using copper-clad diamond powder or its mixture with pure copper powder. Copper-clad diamond is a novel powder consisting of an inside diamond powder, a thin interbedded nickel layer and an outside electroless copper cladding. The sprayed DMMC coatings fabricated using different powders had thickness exceeding 5 mm, i.e. order of magnitude thicker than those typically produced by chemical vapor deposition

(CVD) processes. Due to the low working temperature, the coatings exhibited no phase transformations. In the coatings fabricated from the mixed feedstock of copper and copper-clad diamond, the additional copper powders acted as a buffer, dissipating most of the kinetic energy through the plastic deformation of copper, thereby effectively preventing the fracture of the diamond phase in the coatings. When using pure copper-clad diamond powder as the feedstock only, the impact stress imposed on the diamonds exceeded the diamond fracture stress, leading to a frequent diamond phase fragmentation during the deposition. The pure copper-clad diamond coating was then formed through the bonding between the copper claddings only and the fractured diamond uniformly dispersed into the metal phase. In all coatings, the diamond in the feedstock was fully transferred from the feedstock, with negligible losses only (e.g., reduction from 50 wt% to 43 wt% in the copper-clad diamond coating) – a results never achieved in the previous cold spray works with conventional pre-mixed powders.

Finally, the wear test on the DMMC coating clearly showed that the cold sprayed DMMC coating had superior wear-resistance properties. With copper not being a typical wear-resistance metal, the results clearly reflect the role of the diamond reinforcement in improving the wear-resistance capability. In the future works, copper may be replaced by other wear-resistance metals, such as e.g. cobalt.

Acknowledgments

The authors would like to thank the CRANN Advanced Microscopy Laboratory (AML) of Trinity College for the equipment support, and to Enterprise Ireland (EI) for the financial contribution towards this study. The work of J.C. was supported by Czech Science Foundation project GACR 13-35890S.

References

[1] Wan BQ, Sun XY, Ma HT, Feng RF, Li YS, Yang Q. Plasma enhanced chemical vapor deposition of diamond coatings on Cu–W and Cu–WC composites. Surf Coatings Technol 2015;284:133–8.

337 doi:10.1016/j.surfcoat.2015.06.079.

338 [2] Qin F, Chou YK, Nolen D, Thompson RG. Coating thickness effects on diamond coated cutting tools.
339 Surf Coatings Technol 2009;204:1056–60. doi:10.1016/j.surfcoat.2009.06.011.

340 [3] Che QL, Zhang JJ, Chen XK, Ji YQ, Li YW, Wang LX, et al. Spark plasma sintering of
341 titanium-coated diamond and copper–titanium powder to enhance thermal conductivity of
342 diamond/copper composites. Mater Sci Semicond Process 2015;33:67–75.
343 doi:10.1016/j.mssp.2015.01.041.

344 [4] Abyzov AM, Kruszewski MJ, Ciupiński Ł, Mazurkiewicz M, Michalski A, Kurzydłowski KJ.
345 Diamond–tungsten based coating–copper composites with high thermal conductivity produced by
346 Pulse Plasma Sintering. Mater Des 2015;76:97–109. doi:10.1016/j.matdes.2015.03.056.

347 [5] Shao WZ, Ivanov V V., Zhen L, Cui YS, Wang Y. A study on graphitization of diamond in
348 copper-diamond composite materials. Mater Lett 2004;58:146–9.
349 doi:10.1016/S0167-577X(03)00433-6.

350 [6] Chu K, Liu Z, Jia C, Chen H, Liang X, Gao W, et al. Thermal conductivity of SPS consolidated
351 Cu/diamond composites with Cr-coated diamond particles. J Alloys Compd 2010;490:453–8.
352 doi:10.1016/j.jallcom.2009.10.040.

353 [7] Schubert T, Ciupiński Ł, Zieliński W, Michalski A, Weißgärber T, Kieback B. Interfacial
354 characterization of Cu/diamond composites prepared by powder metallurgy for heat sink applications.
355 Scr Mater 2008;58:263–6. doi:10.1016/j.scriptamat.2007.10.011.

356 [8] Abyzov AM, Kidalov S V., Shakhov FM. High thermal conductivity composite of diamond particles
357 with tungsten coating in a copper matrix for heat sink application. Appl Therm Eng 2012;48:72–80.
358 doi:10.1016/j.applthermaleng.2012.04.063.

359 [9] Feng H, Yu JK, Tan W. Microstructure and thermal properties of diamond/aluminum composites with
360 TiC coating on diamond particles. Mater Chem Phys 2010;124:851–5.
361 doi:10.1016/j.matchemphys.2010.08.003.

362 [10] Kang Q, He X, Ren S, Zhang L, Wu M, Guo C, et al. Preparation of copper-diamond composites with
363 chromium carbide coatings on diamond particles for heat sink applications. Appl Therm Eng

2013;60:423–9. doi:10.1016/j.applthermaleng.2013.05.038.

[11] Li J, Zhang H, Zhang Y, Che Z, Wang X. Microstructure and thermal conductivity of Cu/diamond composites with Ti-coated diamond particles produced by gas pressure infiltration. J Alloys Compd 2015;647:941–6. doi:10.1016/j.jallcom.2015.06.062.

[12] Dong Y, Zhang R, He X, Ye Z, Qu X. Fabrication and infiltration kinetics analysis of Ti-coated diamond/copper composites with near-net-shape by pressureless infiltration. Mater Sci Eng B 2012;177:1524–30. doi:http://dx.doi.org/10.1016/j.mseb.2012.08.009.

[13] Venkateswarlu K, Ray AK, Gunjan MK, Mondal DP, Pathak LC. Tribological wear behavior of diamond reinforced composite coating. Mater Sci Eng A 2006;418:357–63. doi:10.1016/j.msea.2005.12.004.

[14] Richardson AF, Neville A, Wilson JIB. Developing diamond MMCs to improve durability in aggressive abrasive conditions. Wear 2003;255:593–605. doi:10.1016/S0043-1648(03)00049-8.

[15] Venkateswarlu K, Rajinikanth V, Naveen T, Sinha DP, Atiquzzaman, Ray AK. Abrasive wear behavior of thermally sprayed diamond reinforced composite coating deposited with both oxy-acetylene and HVOF techniques. Wear 2009;266:995–1002. doi:10.1016/j.wear.2009.02.001.

[16] Yang L, Li B, Yao J, Li Z. Effects of diamond size on the deposition characteristic and tribological behavior of diamond/Ni60 composite coating prepared by supersonic laser deposition. Diam Relat Mater 2015;58:139–48. doi:10.1016/j.diamond.2015.06.014.

[17] Yao J, Yang L, Li B, Li Z. Beneficial effects of laser irradiation on the deposition process of diamond/Ni60 composite coating with cold spray. Appl Surf Sci 2015;330:300–8. doi:10.1016/j.apsusc.2015.01.029.

[18] Cavaliere P, Perrone A, Silvello A. Mechanical and microstructural behavior of nanocomposites produced via cold spray. Compos Part B Eng 2014;67:326–31. doi:10.1016/j.compositesb.2014.07.023.

[19] Yang GJ, Gao PH, Li CX, Li CJ. Simultaneous strengthening and toughening effects in WC-(nanoWC-Co). Scr Mater 2012;66:777–80. doi:10.1016/j.scriptamat.2012.02.005.

[20] Yang G-J, Gao P-H, Li C-X, Li C-J. Mechanical property and wear performance dependence on

391 processing condition for cold-sprayed WC-(nanoWC-Co). Appl Surf Sci 2015;332:80–8.
392 doi:10.1016/j.apsusc.2015.01.138.

393 [21] Yang GJ, Li CJ, Han F, Li WY, Ohmori A. Low temperature deposition and characterization of TiO2
394 photocatalytic film through cold spray. Appl Surf Sci 2008;254:3979–82.
395 doi:10.1016/j.apsusc.2007.12.016.

396 [22] Lee HY, Yu YH, Lee YC, Hong YP, Ko KH. Interfacial studies between cold-sprayed WO3, Y2O3
397 films and Si substrate. Appl Surf Sci 2004;227:244–9. doi:10.1016/j.apsusc.2003.11.073.

398 [23] Papyrin A. Cold Spray Technology. Adv Mater Process 2001;159:49–51.

399 [24] King PC, Zahiri SH, Jahedi M. Focused ion beam micro-dissection of cold-sprayed particles. Acta
400 Mater 2008;56:5617–26. doi:10.1016/j.actamat.2008.07.034.

401 [25] Melendez NM, Narulkar VV, Fisher GA, McDonald AG. Effect of reinforcing particles on the wear
402 rate of low-pressure cold-sprayed WC-based MMC coatings. Wear 2013;306:185–95.
403 doi:10.1016/j.wear.2013.08.006.

404 [26] Dosta S, Couto M, Guilemany JM. Cold spray deposition of a WC-25Co cermet onto Al7075-T6 and
405 carbon steel substrates. Acta Mater 2013;61:643–52. doi:10.1016/j.actamat.2012.10.011.

406 [27] Yin S, Wang X, Suo X, Liao H, Guo Z, Li W, et al. Deposition behavior of thermally softened copper
407 particles in cold spraying. Acta Mater 2013;61:5105–18. doi:10.1016/j.actamat.2013.04.041.

408 [28] Grujicic M, Zhao CLC, DeRosset WSW, Helfritch D. Adiabatic shear instability based mechanism for
409 particles/substrate bonding in the cold-gas dynamic-spray process. Mater Des 2004;25:681–8.
410 doi:10.1016/j.matdes.2004.03.008.

411 [29] Choi HJ, Lee M, Lee JY. Application of a cold spray technique to the fabrication of a copper canister
412 for the geological disposal of CANDU spent fuels. Nucl Eng Des 2010;240:2714–20.
413 doi:10.1016/j.nucengdes.2010.06.038.

414 [30] Champagne VK. The repair of magnesium rotorcraft components by cold spray. J Fail Anal Prev
415 2008;8:164–75. doi:10.1007/s11668-008-9116-y.

416 [31] Woo DJ, Heer FC, Brewer LN, Hooper JP, Osswald S. Synthesis of nanodiamond-reinforced
417 aluminum metal matrix composites using cold-spray deposition. Carbon N Y 2015;86:15–25.

418 doi:10.1016/j.carbon.2015.01.010.

419 [32] Woo DJ, Sneed B, Peerally F, Heer FC, Brewer LN, Hooper JP, et al. Synthesis of
420 nanodiamond-reinforced aluminum metal composite powders and coatings using high-energy ball
421 milling and cold spray. Carbon N Y 2013;63:404–15. doi:10.1016/j.carbon.2013.07.001.

422 [33] Kim HJ, Jung DH, Jang JH, Lee CH. Study on Metal/Diamond Binary Composite Coatings by Cold
423 Spray. Mater Sci Forum 2007;534–536:441–4. doi:10.4028/www.scientific.net/MSF.534-536.441.

424 [34] Aldwell B, Yin S, Mcdonnell KA, Trimble D, Hussain T, Lupoi R. A novel method for metal –
425 diamond composite coating deposition with cold spray and formation mechanism. Scr Mater
426 2016;115:10–3. doi:10.1016/j.scriptamat.2015.12.028.

427 [35] Melendez NM, McDonald AG. Development of WC-based metal matrix composite coatings using
428 low-pressure cold gas dynamic spraying. Surf Coatings Technol 2013;214:101–9.
429 doi:10.1016/j.surfcoat.2012.11.010.

430 [36] Kumari K, Anand K, Bellacci M, Giannozzi M. Effect of microstructure on abrasive wear behavior of
431 thermally sprayed WC-10Co-4Cr coatings. Wear 2010;268:1309–19. doi:10.1016/j.wear.2010.02.001.

432 [37] Na H, Bae G, Shin S, Kumar S, Kim H, Lee C. Advanced deposition characteristics of kinetic sprayed
433 bronze/diamond composite by tailoring feedstock properties. Compos Sci Technol 2009;69:463–8.
434 doi:10.1016/j.compscitech.2008.11.015.

435 [38] Yin S, Wang XF, Li WY, Jie HE. Effect of substrate hardness on the deformation behavior of
436 subsequently incident particles in cold spraying. Appl Surf Sci 2011;257:7560–5.
437 doi:10.1016/j.apsusc.2011.03.126.

438 [39] Yin S, Zhang M, Guo Z, Liao H, Wang X. Numerical investigations on the effect of total pressure and
439 nozzle divergent length on the flow character and particle impact velocity in cold spraying. Surf
440 Coatings Technol 2013;232:290–7. doi:10.1016/j.surfcoat.2013.05.017.

441 [40] Kwon H, Cho S, Kawasaki A. Diamond-Reinforced Metal Matrix Bulk Materials Fabricated by a
442 Low-Pressure Cold-Spray Process 2015;56:108–12.

443 [41] Shin S, Xiong Y, Ji Y, Kim HJ, Lee C. The influence of process parameters on deposition
444 characteristics of a soft/hard composite coating in kinetic spray process. Appl Surf Sci

2008;254:2269–75. doi:10.1016/j.apsusc.2007.09.017.

[42] Chen LY, Konishi H, Fehrenbacher A, Ma C, Xu JQ, Choi H, et al. Novel nanoprocessing route for bulk graphene nanoplatelets reinforced metal matrix nanocomposites. Scr Mater 2012;67:29–32. doi:10.1016/j.scriptamat.2012.03.013.

[43] Yang N, Boselli J, Sinclair I. Simulation and quantitative assessment of homogeneous and inhomogeneous particle distributions in particulate metal matrix composites. J Microsc 2001;201:189–200. doi:10.1046/j.1365-2818.2001.00766.x.

[44] Iacob G, Ghica VG, Buzatu M, Buzatu T, Petrescu MI. Studies on wear rate and micro-hardness of the Al/Al2O3/Gr hybrid composites produced via powder metallurgy. Compos Part B Eng 2014;69:603–11. doi:10.1016/j.compositesb.2014.07.008.

[45] Yu M, Suo XK, Li WY, Wang YY, Liao HL. Microstructure, mechanical property and wear performance of cold sprayed Al5056/SiCp composite coatings: Effect of reinforcement content. Appl Surf Sci 2014;289:188–96. doi:10.1016/j.apsusc.2013.10.132.

[46] Guo X, Chen J, Yu H, Liao H, Coddet C. A study on the microstructure and tribological behavior of cold-sprayed metal matrix composites reinforced by particulate quasicrystal. Surf Coatings Technol 2015;268:94–8. doi:10.1016/j.surfcoat.2014.05.062.